Note on Dual Solutions for the Mixed Convection Boundary Layer Flow Close to the Lower Stagnation Point of a Horizontal Circular Cylinder: Case of Constant Surface Heat Flux

Nota Dua Penyelesaian bagi Aliran Lapisan Sempadan Perolakan Bercampur Hampir dengan Rendah Silinder Bulat Mendatar: Kes Fluks Haba Permukaan Malar

Alin V. Roşca, Natalia C. Roşca & Ioan Pop*

ABSTRACT

The paper reconsiders the problem of the mixed convection boundary layer flow near the lower stagnation point of a horizontal circular cylinder with a second order slip velocity model and a constant surface heat flux studied recently by Roşca et al. (2013). The ordinary (similarity) differential equations are solved numerically using the function bvp4c from Matlab for different values of the governing parameters. It is found that the similarity equations have two branches, upper and lower branch solutions, in a certain range of the mixed convection parameters. A stability analysis has been performed to show that the upper branch solutions are stable and physically realizable, while the lower branch solutions are not stable and therefore, not physically possible. This stability analysis is different by that presented by Roşca et al. (2013), who have presented a time-dependent analysis to determine the stability of the solution branches.

Keywords: Dual solutions; mixed convection; numerical solution; second-order slip flow; similarity solution; stagnation point

ABSTRAK

Kertas ini mempertimbangkan semula masalah aliran lapisan sempadan perolakan bercampur berhampiran titik genang rendah silinder bulat mendatar dengan model halaju gelincir peringkat kedua dan fluks haba permukaan malar yang dikaji oleh Roşca et al. (2013) sebelum ini. Persamaan pembezaan biasa (keserupaan) diselesaikan secara berangka menggunakan bvp4c fungsi dari Matlab bagi nilai berbeza daripada parameter pengelasan. Adalah didapati bahawa keserupaan persamaan mempunyai dua cabang, penyelesaian cabang atas dan bawah dalam sesetengah julat parameter perolakan bercampur. Analisis kestabilan yang telah dijalankan menunjukkan bahawa penyelesaian cabang atas adalah stabil dan tersedia secara fizikal, manakala penyelesaian cabang bawah adalah tidak stabil dan oleh itu, tidak mungkin tersedia secara fizikal. Analisis kestabilan ini adalah berbeza daripada yang dikemukakan oleh Roşca et al. (2013) yang telah menyampaikan analisis bersandar- masa untuk menentukan kestabilan cabang penyelesaian.

Kata kunci: Dua penyelesaian; halaju gelincir peringkat kedua; penyelesaian berangka; penyelesaian persamaan; perolakan bercampur; titik stagnasi

INTRODUCTION

Forced, free and mixed convection flow is encountered in many practical applications, which include solar central receivers exposed to wind currents, electronic devices cooled by fans, nuclear reactors cooled during emergency shutdown and heat exchangers placed in a low-velocity-environment (Seshadri et al. 2002). This process of heat transfer is also encountered in atmospheric and ocean circulations, in the handling of spent nuclear reactor fuel assemblies, in the design of solar energy collectors and in the process of frost formation involving low temperature surfaces. Hiemenz (1911) is the first who considered the steady two-dimensional forced convection near the stagnation point of a circular cylinder. In the past several years considerable amount of interest has been given to the free and forced convection stagnation point flows of a viscous fluid (Amin & Riley 1995; Ariel 1994; Bian & Rangel 1996; Ramachandran et al. 1988). Convective flows are usually modelled by assuming that the flow is driven either by a prescribed surface temperature or by a prescribed surface heat flux or by Newtonian heating from the bounding surface (Merkin 1994) or by convective surface boundary condition (Aziz 2009; Makinde & Olanrewaju 2010; Merkin & Pop 2011).

All these investigations are done, however, without considering the effect of the velocity slip. The non-adherence of the fluid to a solid boundary, also known as velocity slip, is a phenomenon that has been observed under some assumptions. Wu (2008) proposed a new second order slip velocity model. Thus, Wang (2003) presented exact similarity solutions of the Navier-Stokes equations with slip velocity along a fixed plate. In another

paper he studied the two-dimensional or axisymmetric stagnation flow impinges on a plate moving in its own plane. The no slip condition on the solid boundary is replaced by the partial slip condition (Wang 2006). It has been shown that the Navier–Stokes and energy equations admit exact similarity solutions. The resulting nonlinear differential equations were solved both asymptotically and numerically. He showed that the Navier–Stokes and energy equations admit exact similarity solutions. The resulting nonlinear differential equations are solved asymptotically and numerically. Fang and Lee (2005) presented exact solutions for the flow of a viscous fluid past a stretching sheet with partial slip and also for an incompressible Couette flow with porous walls and slightly rarefied gases (Fang & Lee 2006).

In a recent paper by Roşca et al. (2013) the mixed convection boundary-layer flow near the lower stagnation point of a horizontal circular cylinder with a second-order slip velocity model and a constant surface heat flux has been considered. The transformed ordinary differential (similarity) equations have been solved numerically for different values of the governing parameters. The numerical studies are complemented by the derivation of a time-dependent analysis to determine the stability of the solution branches. We present, however, here a numerical analysis of the dual (upper and lower branch) solutions of the problem considered by Roşca et al. (2013) along with a corresponding numerical stability analysis. The second-order slip velocity considered is similar with that used by Fang et al. (2010) for the flow past a permeable shrinking surface. Therefore, we believe that the present results are different by those given in the paper by Roşca et al. (2013).

BASIC EQUATIONS

Consider the mixed convection problem of a Newtonian fluid near the lower stagnation point of a horizontal circular cylinder of radius a with a velocity slip condition on the wall and a constant wall heat flux q_w, where $q_w > 0$ corresponds to a heated cylinder (assisting flow) and $q_w < 0$ corresponds to a cooled cylinder (opposing flow), respectively, as shown in Figure 1. It is also assumed that the velocity of the outer (inviscid) flow is $U_e(x)$. Under these assumptions, the unsteady boundary-layer equations in the Cartesian coordinates x and y are (Roşca et al. 2013).

$$\frac{\partial u}{\partial x} + \frac{\partial v}{\partial y} = 0. \tag{1}$$

$$\frac{\partial u}{\partial t} + u\frac{\partial u}{\partial x} + v\frac{\partial u}{\partial y} = U_e \frac{dU_e}{dx} + v\frac{\partial^2 u}{\partial y^2} + g\beta\left(T - T_\infty\right)\sin\phi. \tag{2}$$

$$\frac{\partial T}{\partial t} + u\frac{\partial T}{\partial x} + v\frac{\partial T}{\partial y} = \alpha\frac{\partial^2 T}{\partial y^2}, \tag{3}$$

where x is the coordinate measured along the surface of the cylinder started from the lower stagnation point of the
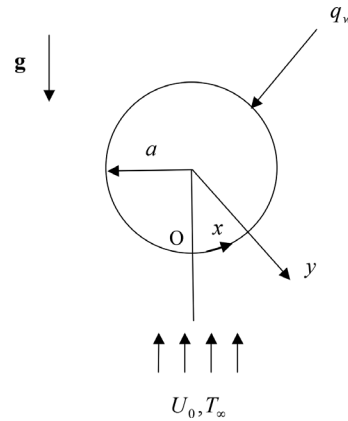

FIGURE 1. Physical model and coordinate system

cylinder and y is the coordinate measured in the direction normal to the surface of the cylinder, respectively, t is the time, u and v are the velocity components along x and y axes, T is the fluid temperature, g is the gravitation acceleration, α is the thermal diffusivity, β is the coefficient of thermal expansion, v is the kinematic viscosity, ϕ is the angle between outward normal at the body surface and the downward vertical. Near the stagnation point we can approximate $\sin\phi \approx x/a$ and the outer (inviscid) flow is approximated by $U_e(x) \approx U_0\, x/a$, where U_0 is the velocity scale. Equations (1-3) are subject to the initial and boundary conditions,

$$t = 0: \quad v = v_0, \quad u = 0, \quad T = T_\infty \quad \text{for any } x, y$$
$$t > 0: \quad v = v_0, \quad u = u_{\text{slip}}, \quad \frac{\partial T}{\partial y} = -\frac{q_w}{k} \text{ at } 0 \leq y < \infty \tag{4}$$
$$u \to U_e(x) = U_0 x/a, \quad T \to T_\infty \text{ as } y \to \infty,$$

where u_{slip} is the velocity slip at the wall, which is valid for arbitrary Knudsen numbers, K_n, and is given as in Fang et al. (2010) and Wu (2008),

$$u_{\text{slip}} = \frac{2}{3}\left(\frac{3 - \bar{\alpha}\ell^2}{\bar{\alpha}} - \frac{3}{2}\frac{1 - \ell^2}{K_n}\right)\delta\frac{\partial u}{\partial y} - \frac{1}{4}$$
$$\left(\ell^4 + \frac{2}{K_n^4}\left(1 - \ell^2\right)\right)\delta^2\frac{\partial^2 u}{\partial y^2} = M\frac{\partial u}{\partial y} + N\frac{\partial^2 u}{\partial y^2}. \tag{5}$$

Here $\ell = \min(1/K_n, 1)$, α is the momentum accommodation coefficient with $0 \leq \bar{\alpha} \leq 1$ and δ is the molecular mean free path. Based on the definition of l, it is seen that for any given value of K_n, we have $0 \leq \ell \leq 1$. The molecular mean free path δ is always positive. Thus we know that $M \geq 0$ and $N \leq 0$. Here T_∞ is the ambient temperature and k is the thermal conductivity.

Following Roşca et al. (2013), the following dimensionless variables are introduced

$$\psi = \frac{v\,\text{Re}^{1/2}}{a}x\, f\left(\bar{y}, \bar{t}\right), \quad T - T_\infty = \frac{q_w a}{k\,\text{Re}^{1/2}}\theta\left(\bar{y}, \bar{t}\right),$$
$$\bar{x} = \frac{x}{a}, \quad y = \frac{\text{Re}^{1/2}}{a}y, \quad \bar{t} = \frac{U_0}{a}t, \tag{6}$$

where Re $= U_0 a/v$ is the Reynolds number and ψ is the stream function, which is defined as $u = \partial\psi/\partial y$ and $v = -\partial\psi/\partial x$. Substituting (6) into (2) and (3) and dropping the overbars, we obtain the following equations,

$$\frac{\partial^3 f}{\partial y^3} + f\frac{\partial^2 f}{\partial y^2} + 1 - \left(\frac{\partial f}{\partial y}\right)^2 + \lambda\theta = \frac{\partial^2 f}{\partial y \partial t}. \tag{7}$$

$$\frac{1}{Pr}\frac{\partial^2\theta}{\partial y^2} + f\frac{\partial\theta}{\partial y} = \frac{\partial\theta}{\partial t}. \tag{8}$$

The initial and boundary conditions (4) become:

$$t = 0: \quad f = 0 \quad \frac{\partial f}{\partial t} = 0, \quad \theta = 0 \quad \text{for any } y$$

$$t > 0: \quad f = 0, \quad \frac{\partial f}{\partial y} = A\frac{\partial^2 f}{\partial y^2} + B\frac{\partial^3 f}{\partial y^3}, \quad \frac{\partial\theta}{\partial y} = -1 \quad \text{at } y = 0$$

$$\frac{\partial f}{\partial y} \to 1, \quad \theta \to 0 \quad \text{as } y \to \infty, \tag{9}$$

where $Pr = v/\alpha$ is the Prandtl number, λ is the mixed convection parameter, A and B are constant dimensionless slip parameters with $A \geq 0$ and $B \leq 0$, which are given by:

$$\lambda = \frac{g\beta(q_w/k)a^2}{U_0^2 Re^{1/2}} = \frac{Gr}{Re^{5/2}}, \quad A = \frac{M Re^{1/2}}{a}, \quad B = \frac{N Re^{1/2}}{a}. \tag{10}$$

Here $Gr = g\,\beta(q_w/k)\,a^4/v^2$ is the Grashof number based on the heat flux q_w. We notice that λ can be either positive (aiding flow), negative (opposing flow) and $\lambda = 0$ corresponds to the forced convection flow, respectively. It should be stated that (7) and (8) describe the classical unsteady mixed convection boundary layer stagnation point flow, which we have to use for the stability of the dual solutions. In addition, it should be mention that the initial and the boundary conditions are new for this problem.

The physical quantities of interest are the skin friction coefficient C_f and the Nusselt number Nu, which are defined as:

$$C_f = \frac{\tau_w}{\rho U_e(x)}, \quad Nu = \frac{aq_w}{k(T_w - T_\infty)}, \tag{11}$$

where τ_w is the skin friction or shear stress along the surface of the cylinder and q_w is the heat flux from the surface of the cylinder, which are given by:

$$\tau_w = \mu\left(\frac{\partial u}{\partial y}\right)_{y=0}, \quad q_w = -k\left(\frac{\partial T}{\partial y}\right)_{y=0}. \tag{12}$$

Using (6), we get

$$Re_x^{1/2} C_f = f''(0), \quad Re^{1/2} Nu = \frac{1}{\theta(0)}, \tag{13}$$

where $Re_x = U_e(x)x/v$ is the local Reynolds number.

STEADY FLOW CASE

The steady states of (7) and (8), which represent the possible large time state of the system, are given by the ordinary differential equations:

$$f''' + f f'' + 1 - f'^2 + \lambda\theta = 0. \tag{14}$$

$$\theta'' + Pr f \theta' = 0, \tag{15}$$

subject to the boundary conditions:

$$f(0) = 0, \quad f'(0) = A f''(0) + B f'''(0), \quad \theta'(0) = -1$$
$$f'(y) \to 1, \quad \theta(y) \to 0 \quad \text{as } y \to \infty, \tag{16}$$

where primes denote differentiation with respect to y. It is worth to mention that when $\lambda = A = B = 0$, the problem becomes the classical steady stagnation point flow, described by Hiemenz (1911).

FLOW STABILITY

In order to test the stability of the steady flow solution $f(y) = f_0(y)$ and $\theta(y) = \theta_0(y)$, which satisfy the boundary-value problem (14-16), we write (Merkin 1985; Roşca & Pop 2013; Weidman et al. 2006),

$$f(y,t) = f_0(y) + e^{-\gamma t} F(y,t), \quad \theta(y,t) = \theta_0(y) + e^{-\gamma t} G(y,t), \tag{17}$$

where γ is an unknown eigenvalue parameter and $F(y, t)$ and $G(y, t)$ are small relative to $f_0(y)$ and $\theta_0(y)$. After substituting (17) into (7) and (8), we arrive to the following linearized problem,

$$\frac{\partial^3 F}{\partial y^3} + f_0\frac{\partial^2 F}{\partial y^2} + f_0'' F - 2f_0'\frac{\partial F}{\partial y} + \gamma\frac{\partial F}{\partial y} + \lambda G = \frac{\partial^2 F}{\partial y \partial t}. \tag{18}$$

$$\frac{1}{Pr}\frac{\partial^2 G}{\partial y^2} + f_0\frac{\partial G}{\partial y} + F\theta_0' + \gamma G = \frac{\partial G}{\partial t}, \tag{19}$$

along with the boundary conditions,

$$F(0,t) = 0, \quad \frac{\partial F}{\partial y}(0,t) = A\frac{\partial^2 F}{\partial y^2}(0,t) + B\frac{\partial^3 F}{\partial y^3}(0,t),$$

$$\frac{\partial G}{\partial y}(0,t) = 0 \tag{20}$$

$$\frac{\partial F}{\partial y}(y,t) \to 0, \quad G(y,t) \to 0 \quad \text{as } y \to \infty.$$

As in Merkin (1985), we analyse the stability of the steady flow and heat transfer solution $f_0(y)$ and $\theta_0(y)$ by setting $t = 0$. Thus, $F = F_0(y)$ and $G = G_0(y)$ in (18) and (19) identify initial growth or decay of the solution (17). This leads to the following linear eigenvalue problem

$$F_0''' + f_0 F_0'' + f_0'' F_0 - \left(2f_0' - \gamma\right)F_0' + \lambda G_0 = 0. \tag{21}$$

$$\frac{1}{Pr}G_0'' + f_0 G_0' + F_0\theta_0' + \gamma G_0 = 0, \tag{22}$$

along with the boundary conditions,

$$F_0(0) = 0, \quad F_0'(0) = A F_0''(0) + B F_0'''(0), \quad G_0'(0) = 0$$
$$F_0'(y) \to 0, \quad G_0(y) \to 0 \quad \text{as} \quad y \to \infty. \tag{23}$$

It is known that the stability of the corresponding steady flow solution $f_0(y)$ and $\theta_0(y)$ is determined by the smallest eigenvalue γ. Following Harris et al. (2009), the range of possible eigenvalues can be determined by relaxing a boundary condition on $F_0(y)$ or $G_0(y)$. Thus, we relax the condition that $G_0(y) \to 0$ as $y \to \infty$ and for a fixed value of γ we solve the system (21), (22) along with the new boundary condition $G_0(0) = 1$.

NUMERICAL METHOD AND RESULTS

The systems of (14-16) and (21-23) can be solved numerically by several numerical methods such as Keller-box and finite-difference. However, we solved these equations here numerically using the function bvp4c from Matlab, because it works very efficiently for the flow stability. At the beginning, (14-16) and (21-23) are written as a system of first order ordinary differential equations. In general, the bvp4c function implements a collocation method for the solution of the following boundary value problem,

$$y' = f(x, y), \quad a \le x \le b, \tag{24}$$

subject to the two-point boundary conditions:

$$bc(y(a), \ y(b)) = 0. \tag{25}$$

The approximate solution $S(x)$ is a continuous cubic polynomial function on each subinterval $[x_n, x_{n+1}]$ of the mesh $a = x_0 < x_1 < \ldots < x_N = b$ and it satisfies the boundary conditions,

$$bc(S(a), \ S(b)) = 0. \tag{26}$$

The solution $S(x)$ is a fourth order approximation to an isolated solution $y(x)$ of the boundary value problem (24-25), i.e., $\|y(x) - S(x)\| \le A h^4$, where h is the maximum of the step sizes $h_n = x_{n+1}, n = \overline{0, N-1}$ and A is a constant. For such an approximation, the residual $R(x)$ in the ODEs is defined as,

$$R(x) = S'(x) - f(x, S(x)). \tag{27}$$

The relative tolerance was set to 10^{-7} and finite values of $\eta \to \infty$, namely $\eta = \eta_\infty = 10$ for the first solution branch and $\eta = \eta_\infty = 100$ for the second solution branch, respectively, have been chosen. The numerical computations have been carried out for several values of the governing parameters, such as mixed convection parameter λ and of the slip parameters A and B as in Fang et al. (2010). The value of the Prandtl number Pr is taken as Pr = 1. It is found that the

solution of (14) and (15) subject to the boundary conditions (16) is unique for $\lambda > 0$ (assisting flow). However, the case of buoyancy opposing flow ($\lambda < 0$), is considered here. We have validated the accuracy of the numerical scheme, by comparing the obtained results corresponding to the reduced skin friction coefficient $f''(0)$ with the results reported by Wang (2006, 2003) when $B = 0$ (second-order slip is absent) and $\lambda = 0$ (forced convection flow). When $\lambda = A = B = 0$, the problem reduces to the steady stagnation point flow, described by Hiemenz (1911), which reported for $f''(0)$ the value of $f''(0) = 1.2325$, which is in agreement with the value obtained in this paper. These comparisons are shown in Table 1 and it is found that the results are in excellent agreement. It gives us, therefore, the confidence that the present results are accurate.

TABLE 1. Comparison of the values of $f''(0)$ for several values of A when $\lambda = 0$ (forced convection) and $B = 0$

A	$f''(0)$ Present study	$f''(0)$ Wang (2003) or Wang (2006)
0	1.2325 (1.2325)	1.2325
0.2	1.0425	1.0425
0.4	0.8863	0.8863
0.6	0.7642	0.7642
0.8	0.6689	0.6689
1	0.5934	0.5934
2	0.3758	0.3759
5	0.1772	0.1773
10	0.0940	0.0940
20	0.0484	0.0485
50	0.0197	0.0198
∞	0	0

( ) Result by Hiemenz (1911)

Figures 2 and 3 show the variation of the reduced skin friction coefficient $f''(0)$ and $1/\theta(0)$ with λ when $A = B = 0$ (no slip). It is worth mentioning that the results presented in Figure 2 are in completely agreement with the results presented by Roşca et al. (2013). This is also available for Figure 3, where we have plotted $1/\theta(0)$, while Roşca et al. (2013) have plotted $\theta(0)$. Figures 4 and 5 show the variations $f''(0)$ and $1/\theta(0)$ with the mixed convection parameter λ for several values of the first order slip parameter A when the second order slip parameter $B = 0$. Also, Figures 6 to 9 indicate the variation of $f''(0)$ and $1/\theta(0)$ with λ for several values of the parameter B when $A = 0$. However, Figures 6 and 7 are for small absolute values of B, while Figures 8 and 9 are for large absolute values of B. All these figures show that dual solutions (upper and lower branch solutions) exist for (14) and (15)
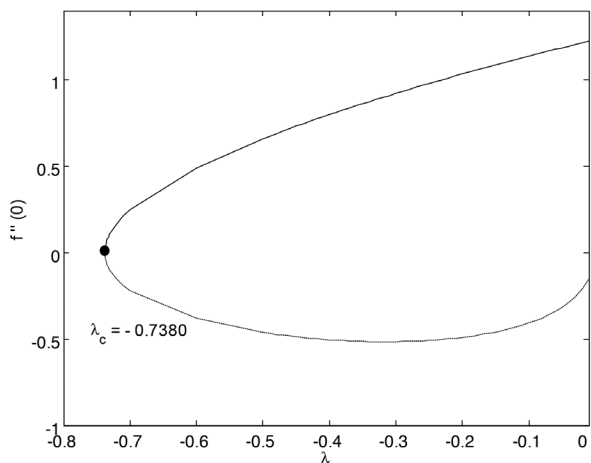
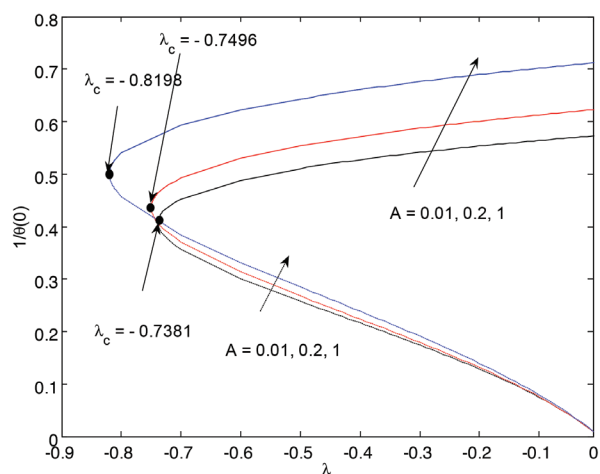FIGURE 2. Variation of $f''(0)$ with λ when $A = 0$ and $B = 0$

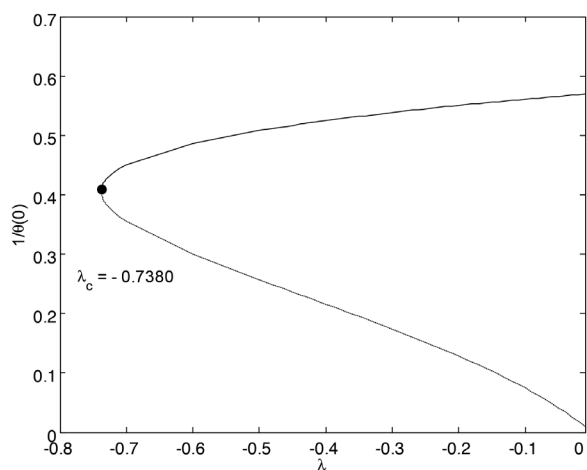FIGURE 5. Variation of $1/\theta(0)$ with λ for several values of A when $B = 0$

FIGURE 3. Variation of $1/\theta(0)$ with λ when $A = 0$ and $B = 0$
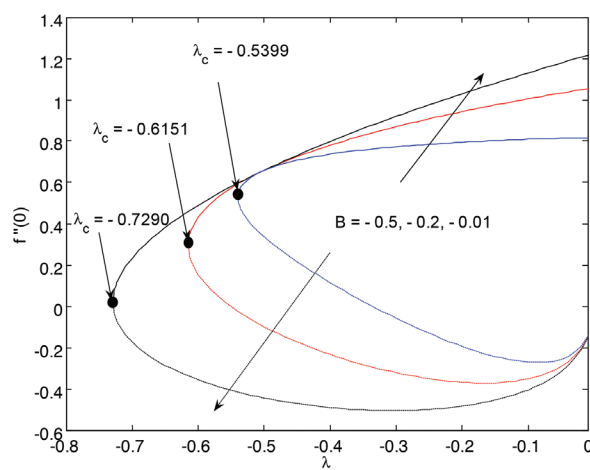
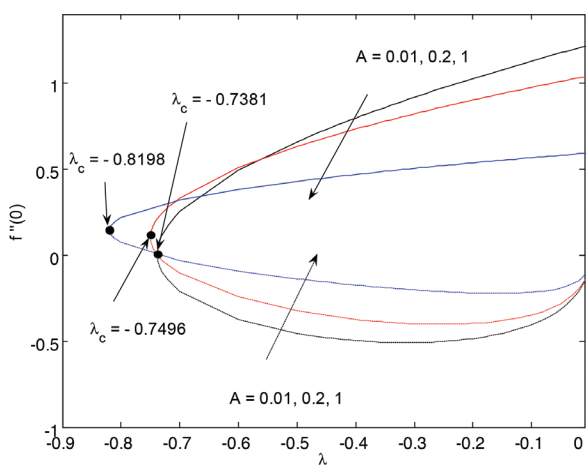FIGURE 6. Variation of $f''(0)$ λ for several values of B when $A = 0$

FIGURE 4. Variation of $f''(0)$ with λ for several values of A when $B = 0$
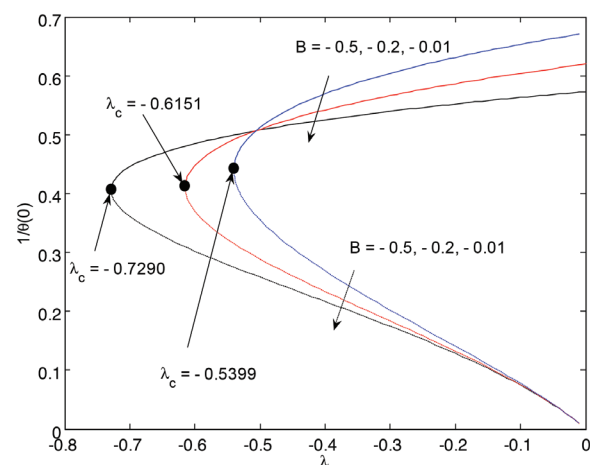
FIGURE 7. Variation of $1/\theta(0)$ with λ for several values of B when $A = 0$
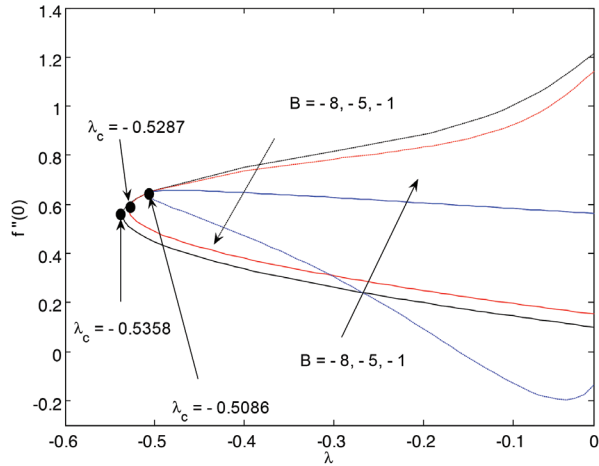
FIGURE 8. Variation of $f''(0)$ with λ for several values of B when $A = 0$
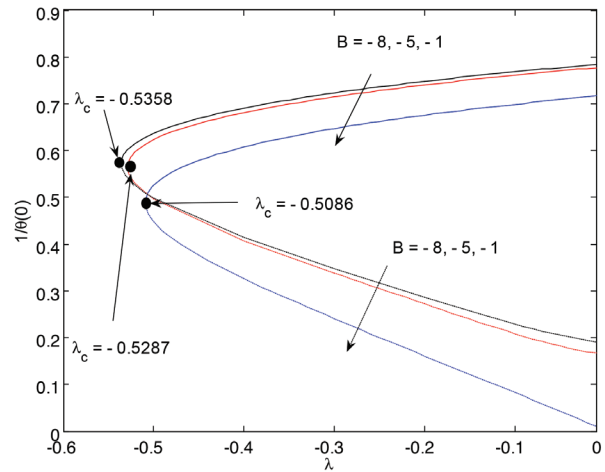

FIGURE 9. Variation of $1/\theta(0)$ with λ for several values of B when $A = 0$

with the boundary conditions (16) for $\lambda_c \leq \lambda \leq 0$ (opposing flow) and no solutions exist for $\lambda < \lambda_c < 0$, where $\lambda_c < 0$ is the critical value of $\lambda < 0$ for which (14) and (15) with the boundary conditions (16) have no solutions. Thus, for $\lambda < \lambda_c < 0$ the full Navier–Stokes and energy equations have to be solved. It has been shown in the paper by Roşca et al. (2013) that when $B = 0$ increasing the value of A, the value of $\lambda_c < 0$ will asymptotically decreas to around -0.95. This is clearly seen also in Figures 4 and 5. As regards Figures 6 to 9 when $A = 0$ and $B < 0$ the value of $\lambda_c < 0$ will increase until about -0.5 in the case of small B and then decreases asymptotically for larger B until about -0.55, which is in completely agreement with the results presented in the paper by Roşca et al. (2013).

In Table 2, we give the smallest eigenvalues γ at several values of $\lambda < 0$ (opposing flow) and of the slip parameters A and B. The stability analysis shows that the upper branch solutions are stable and physically realizable, while the lower branch solutions are unstable and, therefore, not physically realizable (Merkin 1985; Roşca & Pop 2013; Weidman et al. 2006). Such kind of dual solutions have been first studied by Merkin (1985) for the mixed convection flow past a vertical plate embedded in a porous medium and also by Weidman et al. (2006) for the forced convection flow over a permeable moving semi-infinite flat plate.

An analogue further discussion with the results presented by Fang et al. (2010) is given in Figures 4 to 9,

TABLE 2. Smallest eigenvalues γ at several values of λ (< 0, opposing flow), A and B

A	B	λ	Upper branch γ	Lower branch γ
		-0.3	0.5494	-0.5694
0.2	0			
		-0.5	0.4119	-0.4274
		-0.3	0.6788	-0.6662
1	0			
		-0.5	0.5336	-0.5352
		-0.3	0.4985	-0.5016
0	-0.2			
		-0.5	0.3006	-0.3021
		-0.3	0.5569	-0.5272
0	-1			
		-0.5	0.1152	-0.1155
		-0.3	0.6833	-0.6893
1	-1			
		-0.5	0.4648	-0.4765

which illustrate the effects of the slip parameters A and B on $f''(0)$ and $1/q(0)$. However, the results by Fang et al. (2010) are given for the forced convection flow past a shrinking sheet with the second-order slip flow. But the present results are for the mixed convection boundary layer stagnation point flow. Thus, in the case of stable solution, $f''(0)$ decreases monotonically with $A \neq 0$ when the parameter $B = 0$ (Figure 4), while opposite behaviour is noticed from Figures 6 and 8 when $B \neq 0$ and $A = 0$. It is observed from Figure 5 that $1/\theta(0)$ increases monotonically with $A \neq 0$ when the parameter $B = 0$. Opposite behaviour is noticed from Figures 7 and 9 when $B \neq 0$ and $A = 0$. However, on the lower branch solution both $f''(0)$ and $1/\theta(0)$ increase with the parameter $A \neq 0$ when $B = 0$ (Figures 4 and 5), while opposite behaviour is noticed from Figures 6 to 9 when $B \neq 0$ and $A = 0$. Therefore, the slip has a substantial effect on $f''(0)$ and $1/\theta(0)$. Figures 4 to 9 also show that the critical value $|\lambda_c|$ increases as the parameters A and B are increasing, suggesting that the slip increases the range of existence of the solutions of (14) and (15) with the boundary conditions (16).

Finally, Figures 10 to 15 show the samples of velocity $f'(\eta)$ and temperature $\theta(\eta)$ profiles for opposing flow ($\lambda < 0$). One can see that the far field boundary conditions (16) are approached asymptotically and this supports the numerical results obtained. Therefore, the velocity profiles for the stable solution at the plate surface $f'(0)$ are positive when $A > 0$ and $B = 0$ (Figure 10), which is in agreement with the fact that $f''(0)$ is positive (14). The same argument holds for the case $A = 0$ and $B < 0$ (Figure 12). On the other hand, it is clearly seen from these figures that for both velocity and temperature profiles the upper branch solution displays a thinner boundary layer thickness compared to the lower branch solution. The physical importance of this problem consists in that it shows that in the case of dual solutions the flow separates from the plate, which is very important for many practical problems. An improved understanding of such flows and the application of this knowledge to new design techniques should provide substantial improvements in performance, reliability, and costs of many fluid dynamic devices (McCroskey 1977).
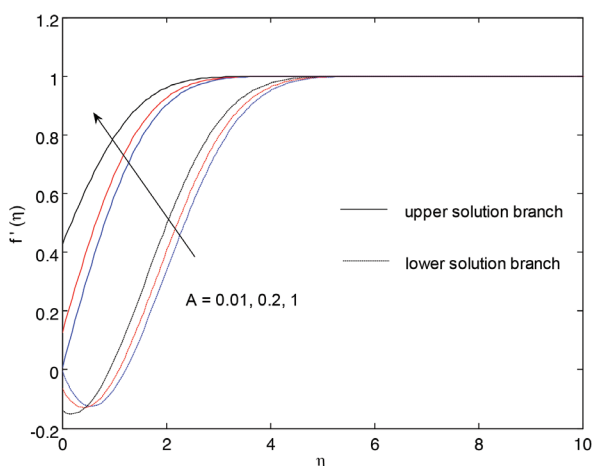

FIGURE 10. Dimensionless velocity $f'(\eta)$ profiles for several values of A when $B = 0$ and $\lambda = -0.5$
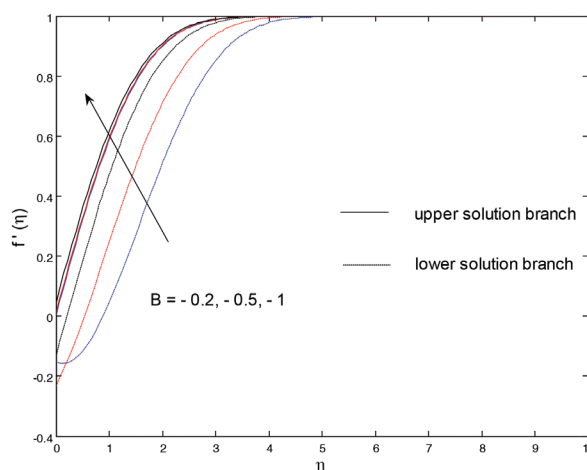

FIGURE 12. Dimensionless velocity $f'(\eta)$ profiles for several values of B when $A = 0$ and $\lambda = -0.5$
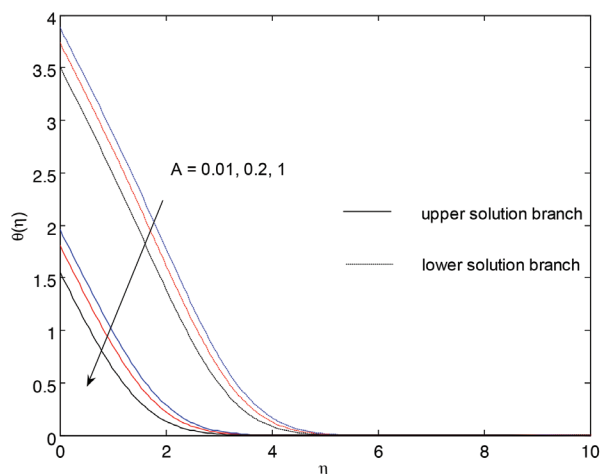

FIGURE 11. Dimensionless temperature $\theta(\eta)$ profiles for several values of A when $B = 0$ and $\lambda = -0.5$
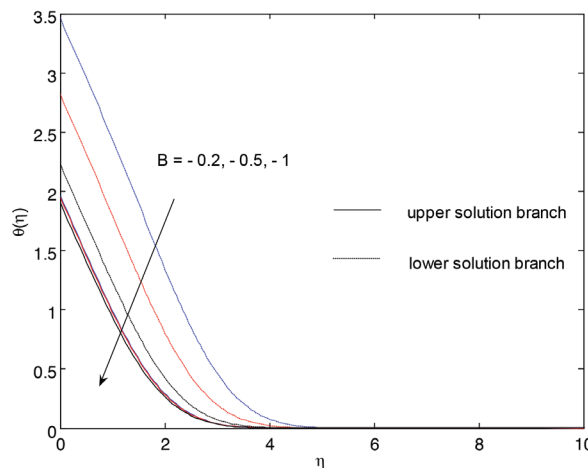

FIGURE 13. Dimensionless temperature $\theta(\eta)$ profiles for several values of B when $A = 0$ and $\lambda = -0.5$
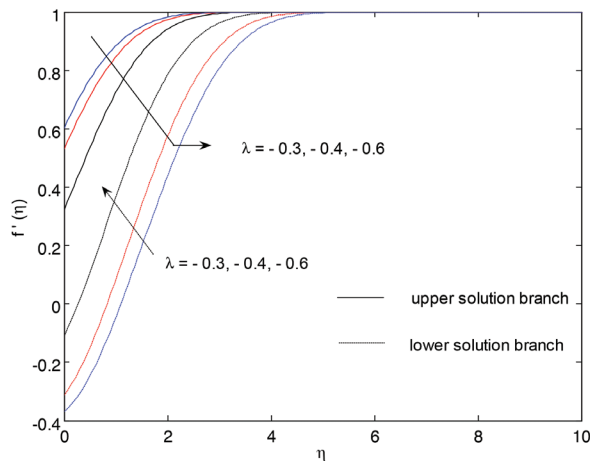
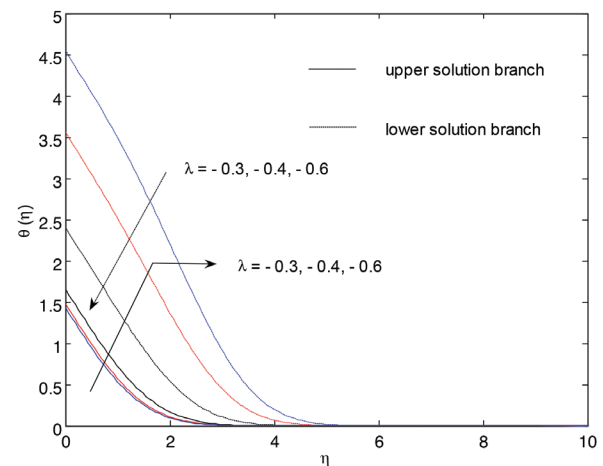FIGURE 14. Dimensionless velocity $f'(\eta)$ profiles for several values of λ when $A = 1$ and $B = -1$

FIGURE 15. Dimensionless temperature $\theta(\eta)$ profiles for several values of λ when $A = 1$ and $B = -1$

CONCLUSION

The problem of the mixed convection boundary layer flow near the lower stagnation point of a horizontal circular cylinder with a constant surface heat flux has been studied in this paper, using a second order velocity slip model. The governing ordinary differential equations (boundary layer equations) were solved numerically for the case of opposing flow regime using the bvp4c method from Matlab. We can draw the following conclusions:

Equations (14) to (16) possess dual solutions for opposing flow case ($\lambda < 0$ and the solution curves bifurcate at the critical values $\lambda_c < 0$. The reduced skin friction coefficient $f''(0)$ decreases monotonically for the upper branch solution with the first order slip parameter $A \neq 0$ when the second order slip parameter is absent ($B = 0$). Opposite behaviour is noticed when $B \neq 0$ and $A = 0$ (first order slip is absent). In the case of $1/\theta(0)$ it increases monotonically with parameter $A \neq 0$ when $B = 0$, while opposite behaviour is noticed when $B \neq 0$ and $A = 0$. However, on the lower branch solution, both $f''(0)$ and $1/\theta(0)$ increase with the parameter $A \neq 0$ when $B = 0$, while opposite behaviour happens when $B \neq 0$ and $A = 0$.

REFERENCES

Amin, N. & Riley, N. 1995. Mixed convection at a stagnation point. *Quart. J. Mech. Appl. Math.* 48: 111-121.

Ariel, P.D. 1994. Stagnation point flow with suction: An approximate solution. *ASME J. Appl. Mech.* 61: 976-978.

Aziz, A. 2009. A similarity solution for laminar thermal boundary layer over flat plate with convective surface boundary condition. *Commun Non. Sci. Numer Simulat.* 14: 1064-1068.

Bian, X. & Rangel, R. H. 1996. The viscous stagnation flow solidification problem. *Int. J. Heat Mass Transfer* 39: 3581-3594.

Fang, T. & Lee, C.F. 2005. A moving-wall boundary layer flow of a slightly rarefied gas free

stream over a moving flat plate. *Appl. Math. Lett.* 18: 487-495.

Fang, T. & Lee, C.F. 2006. Exact solutions of incompressible Couette flow with porous walls for slightly rarefied gases. *Heat Mass Transfer* 42: 255-262.

Fang, T., Yao, S., Zhang, J. & Aziz, A. 2010. Viscous flow over a shrinking sheet with a second order slip flow model. *Commun. Nonlinear Sci. Numer. Simulat.* 15: 1831-1842.

Harris, S.D., Ingham, D.B. & Pop, I. 2009. Mixed convection boundary-layer flow near the stagnation point on a vertical surface in a porous medium: Brinkman model with slip. *Transport Porous Media* 77: 267-285.

Hiemenz, K. 1911. Die Grenzschicht an einem in den gleichformigen Flssigkeitsrom eingetauchten geraden Kreiszylinder. *Dinglers Polytech. J.* 326: 321-324.

Makinde, O.D. & Olanrewaju, P.O. 2010. Buoyancy effects on the thermal boundary layer over a vertical flat plate with a convective surface boundary conditions. *ASME Fluid Eng.* 132: 044502-1 -044502-4.

McCroskey, W.J. 1977. Some current research in unsteady fluid dynamics - The 1976

Freeman scholarship lecture. *ASME Journal of Fluid Engineering* 99: 8-39.

Merkin, J.H. 1985. On dual solutions occurring in mixed convection in a porous medium.

J. Eng. Math. 20: 171-179.

Merkin, J.H. & Pop, I. 2011. The forced convection flow of a uniform stream over a flat surface with a convective surface boundary condition. *Commun. Nonlinear Sci. Numerical Simul.* 16: 3602-3609.

Ramachandran, N., Chen, T.S. & Armaly, B.F. 1988. Mixed convection in stagnation flows adjacent to vertical surfaces. *ASME J. Heat Transfer* 110: 373-377.

Roşca, A.V. & Pop, I. 2013. Flow and heat transfer over a vertical permeable stretching/

shrinking sheet with a second order slip. *Int. J. Heat Mass Transfer* 60: 355-364.

Roşca, N.C., Roşca, A.V., Merkin, J.H. & Pop, I. 2013. Mixed convection boundary-layer flow near the lower stagnation point of a horizontal circular cylinder with a second-order wall velocity condition and a constant surface heat flux. *The IMA Journal of Applied Mathematics*. doi:10.1093/imamat/hxt045 (in press, 2014).

Seshadri, R., Sreeshylan, N. & Nath, G. 2002. Unsteady mixed convection flow in the stagnation region of a heated vertical plate due to impulsive motion. *Int. J. Heat Mass Transfer* 45: 1345-1352.

Wang, C.Y. 2003. Stagnation flows with slip: Exact solutions of the Navier-Stokes Equations. *J. Appl. Math. Phys. (ZAMP)* 54: 184-189.

Wang, C.Y. 2006. Stagnation slip flow and heat transfer on a moving plate. *Chem. Engng. Sci.* 61: 7668-7672.

Weidman, P.D., Kubitschek, D.G. & Davis, A.M.J. 2006. The effect of transpiration on self-similar boundary layer flow over moving surfaces. *Int. J. Engng. Sci.* 44: 730-737.

Wu, L. 2008. A slip model for rarefied gas flows at arbitrary Knudsen number. *Appl. Phys. Lett.* 93: 253103.

Alin V. Roşca
Faculty of Economics and Business Administration
Department of Statistics, Forecasts and Mathematics
Babeş-Bolyai University
R-400084 Cluj-Napoca
Romania

Natalia C. Roşca & Ioan Pop*
Faculty of Mathematics and Computer Science
Department of Mathematics, Babeş-Bolyai University
R-400084 Cluj-Napoca
Romania

*Corresponding author; email: popm.ioan@yahoo.co.uk